*Original Manuscript*

progress in Reaction Kinetics and Mechanism

Progress in Reaction Kinetics and Mechanism
Volume 46: 1–19

DOI: 10.1177/14686783211027446
journals.sagepub.com/home/prk
SAGE

# Understanding the reaction mechanism of the regioselective piperidinolysis of aryl 1-(2,4-dinitronaphthyl) ethers in DMSO: Kinetic and DFT studies

**Yasmen M Moghazy[1], Nagwa MM Hamada[1], Magda F Fathalla[2], Yasser R Elmarassi[1,3], Ezzat A Hamed[2] and Mohamed A El-Atawy[2,4]**

**Abstract**

Reactions of aryl 1-(2,4-dinitronaphthyl) ethers with piperidine in dimethyl sulfoxide at 25°C resulted in substitution of the aryloxy group at the ipso carbon atom. The reaction was measured spectrophotochemically and the kinetic studies suggested that the titled reaction is accurately third order. The mechanism is began by fast nucleophilic attack of piperidine on C1 to form zwitterion intermediate **(I)** followed by deprotonation of zwitterion intermediate **(I)** to the Meisenheimer ion **(II)** in a slow step, that is, SB catalysis. The regular variation of activation parameters suggested that the reaction proceeded through a common mechanism. The Hammett equation using reaction constant $\sigma^{o}$ values and Brønsted coefficient value showed that the reaction is poorly dependent on aryloxy substituent and the reaction was significantly associative and Meisenheimer intermediate-like. The mechanism of piperidinolysis has been theoretically investigated using density functional theory method using B3LYP/6-311G(d,p) computational level. The combination between experimental and computational studies predicts what mechanism is followed either through uncatalyzed or catalyzed reaction pathways, that is, SB and SB-GA. The global parameters of the reactants, the proposed activated complexes, and the local Fukui function analysis explained that $C_1$ carbon atom is the most electrophilic center of ether. Also, kinetics and theoretical calculation of activation energies indicated that the

[1]Chemistry Department, Faculty of Education, Alexandria University, Alexandria, Egypt
[2]Chemistry Department, Faculty of Science, Alexandria University, Alexandria, Egypt
[3]Basic Science Department, Imam Abdulrahman Bin Faisal University (Dammam University), Dammam, Kingdom of Saudi Arabia
[4]Chemistry Department, Faculty of Science, Taibah University, Yanbu, Saudi Arabia

**Corresponding author:**
Magda F Fathalla, Chemistry Department, Faculty of Science, Alexandria University, P.O. 426 Ibrahimia, Alexandria 21321, Egypt.
Email: mffathalla@hotmail.com

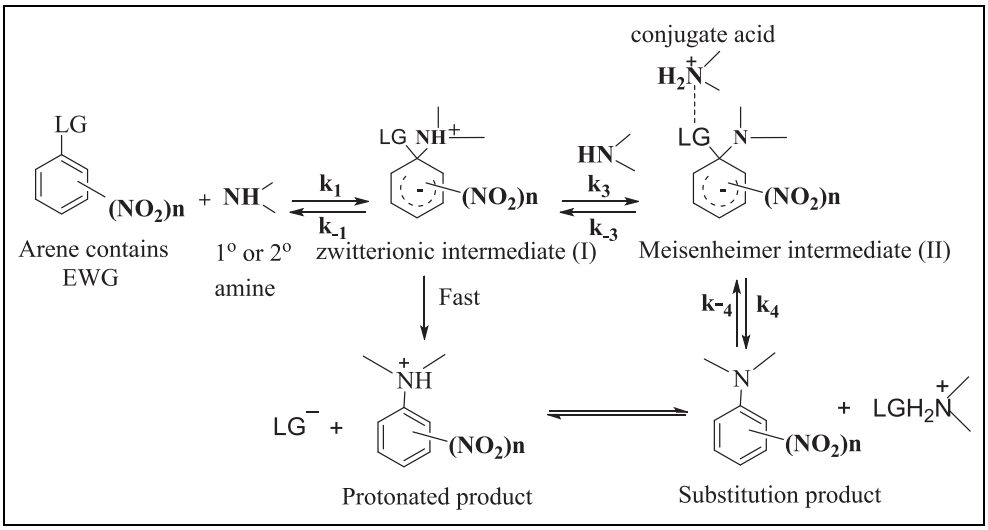


**Scheme 1.** Base catalyzed and uncatalyzed Mechanism of aminolysis of aromatic nitro compounds containing leaving group.

mechanism of the piperidinolysis passed through a two-step mechanism and the proton transfer process was the rate determining step.

**Keywords**
Kinetics, DMSO, DFT Study, aryl 1-(2,4-dinitronaphthyl) ethers, piperidinolysis

## Introduction

The reactions of piperidine with aromatic nitro compounds containing poor leaving group in dimethyl sulfoxide (DMSO) have been reported to subject base catalysis.[1–5] The uncatalyzed pathway proceeded by slow formation of zwitterion followed by fast step to the protonated product which equilibrated with the substitution product (Scheme 1). The catalysis has been reported to be either the slow proton transfer step,[6] that is, specific base (SB)[2,7–13] or the rate-limiting step is the removing of the leaving group by assistance of the conjugate acid,[9,14–18] SB-GA (Scheme 1). The change in rate controlling step has been reported to be dependent on the base strength and the basicity of the leaving group.[9,19] The differentiation between the two pathways mechanism of catalysis is achieved using external base related to SB catalysis and conjugate acid of the same amine used in the reaction related to SB-GA catalysis.

Several studies have been reported that aryl 1-(2,4-dinitronaphthyl) ether **(1a–h)** were considered as good substrates toward SNAr reactions.[20–33] This is because 2,4-dinitro groups with respect to 1-chloro substituent in one of the two rings of naphthalene made it susceptible toward nucleophilic substitution, and stable activated complex(s) is formed.[34,35] In the present study, kinetic of the reaction of aryl 1-(2,4-dinitronaphthyl) ether **(1a–h)** (Ar = **a**, X = H; **b**, X = 4-$OCH_3$; **c**, X = 4-$CH_3$; **d**, X = 3-$CH_3$; **e**, X = 3-$OCH_3$;**f**, X = 4-Cl; **g**, X = 3-Cl; and **h**, X = 4-$NO_2$) with piperidine **(2)** in DMSO at 25°C was examined

experimentally (equation (1)). In addition, intermediates and transition states associated with the rate determining step (RDS) were explored computationally using B3LYP/6-311G(d,p) density functional method. The comparison between experimental and computational studies is used to predict what pathway for the reaction was followed either through uncatalyzed or catalyzed reaction pathways and between SB and SB-GA catalysis (Scheme 1).

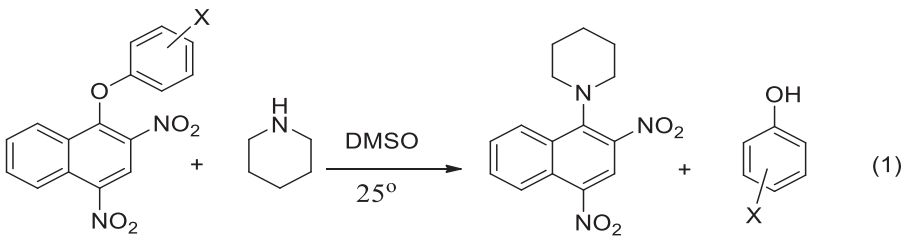


a, X = H; b, X = 4-$OCH_3$; c, X = 4-$CH_3$; d, X = 3-$CH_3$; e, X = 3-$OCH_3$; f, X = 4-Cl; g, X = 3-Cl; h, X = 4-$NO_2$

## Experimental

### *Preparation of aryl 1-(2,4-dinitronaphthalen-1-yl) piperidine (3)*

The reaction 1-aryl 2,4-dinitro-1-naphthyl ethers **(1a–h)** and piperidine **(2)** in DMSO yielded the 1-(N-piperidinyl)-2,4-dinitronapthalene **(3)**.[10,11]

### *Kinetic technique*

*Spectrophotometric studies.* The reaction of 1-aryl 2,4-dinitronaphthyl ether **(1a–h)** with piperidine **(2)** in DMSO was followed spectrophotometrically. The recorded spectral of kinetic reaction was identical to those of the authentic reaction products **(3)** under investigation in the same solvents.

*Kinetic measurements.* A solution of **(1a–h)** ($1 \times 10^{-4}$ M) in 10 ml DMSO was prepared. The reaction time started when the piperidine with concentration ranged from 0.006 to 0.6 M was transferred quickly to a well thermostated chamber containing the ultraviolet (UV) cell. The reaction also was carried out with various concentrations of piperidine in the presence or the absence of pyridine or *p*-toluidinium hydrochloride. The absorbance $A_t$ at the desired $\lambda$ = 440 nm was recorded at several time intervals depending on the reaction rate. The resultant change of absorbance with time was recorded on a JASCO V-530, UV-VIS Spectrophotometer, Japan.

*Method of calculations.* All computational calculations had been performed on personal computer using the Gaussian 09W program packages and 6.31G(d,p) basis set[36] Gaussian output files were visualized by means of Gaussian view 05 software.[37] Computation provided useful information about the optimized molecular structures of **(1a–h)**, piperidine (**2**), and all

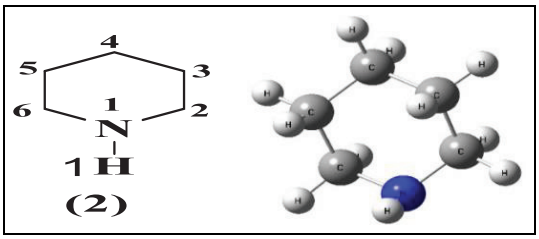


**Figure 1.** Optimized geometry and numbering of piperidine (2).

**Table 1.** Optimized geometrical parameters of piperidine (2) obtained by B3LYP/6-311G(d,p) density functional calculations.

| Bond length (Å) | B3LYP/6-311 G(d,p) | Bond angles (°) | B3LYP/6-311 G(d,p) | Dihedral angles (°) | B3LYP/ 6-311 G(d,p) |
|---|---|---|---|---|---|
| $N_1$–$H_1$ | 1.017 | $C_2$–$N_1$–$C_6$ | 112.3° | $H_1N_1C_1$ $C_2$ | –68.4° |
| $C_1$–$N_1$ ($C_6$–$N_1$) | 1.467 | $N_1$–$C_2$–$C_3$ ($C_5$–$C_6$–$N_1$) | 114.2° | $H_1N_1C_6$ $C_5$ | 68.4 ° |
| $C_2$–$C_3$ ($C_5$–$C_6$) | 1.538 | $C_2$–$C_3$–$C_4$ ($C_6$–$C_5$–$C_4$) | 110.8° | | |
| $C_3$–$C_4$ ($C_4$–$C_5$) | 1.536 | $H_1$–$N_1$–$C_2$ ($H_1$–$N_1$–$C_6$) | 109.1° | | |

possible activated complexes (transition states and intermediates) and their parameters have been assessed to suggest the correct pathway for the reaction under investigation.

## Discussion

### *Structure determination of 1-(N-piperidinyl)-2,4-dinitronaphthalene, 3*

The reaction between ethers (**1a**–**h**: **a**, X = H; **b**, X = 4-$OCH_3$; **c**, X = 4-$CH_3$;**d**, X = 3-$CH_3$; **e**, X = 3-$OCH_3$;**f**, X = 4-Cl; **g**, X = 3-Cl; and **h**, X = 4-$NO_2$) and piperidine **(2)** in DMSO yielded the expected 1-(N-piperidinyl)-2,4-dinitronaphthalene **(3)** and substituted phenol **(4)** with no side products detected independent on the nature of the aryl moiety (equation (1)). The structure of the substitution product **(3)** indicated that the reaction was regioselective and piperidine attached itself to the ipso carbon atom of naphthyl moiety and substituted phenols were the leaving groups.[10,11]

*Optimized geometry of piperidine, (2).* Piperidine molecule is a heterocyclic amine and has two possible chair conformations.[38,39] The calculated and experimental vibrational modes of piperidine had been reported.[40–47] The optimized geometric parameters (bond lengths and angles) by BLYP with 6-311G(d,p) are in accordance with the atom numbering given in Figure 1 and Table 1.

*Molecular orbital analysis of piperidine (2) and (1a–h).* The density functional theory (DFT)[48] was used to understand the chemical reactivity and site selectivity of 1-(2,4-dinitronaphthyl) ether **(1a–h)** and piperidine **(2)**. Accordingly, the values of Mulliken charge, natural bond orbital

**Table 2.** Mulliken charge, NBO charge, and atomic orbital coefficient of HOMO in piperidine (2).

| Atom | Mulliken charge | NBO charge | Atomic orbital coefficient of HOMO |
|---|---|---|---|
| Nitrogen atom | −0.365 | −0.665 | 0.6751 |

NBO: natural bond orbital; HOMO: highest occupied molecular orbital.

**Table 3.** Calculated energies and related molecular properties values of piperidine (2) by B3LYP/6-311G(d,p).

| (2) | $E_{HOMO}$ | $E_{LUMO}$ | ΔEe | $I_P$ | $E_A$ | χ | μ | η | S | ω | $\Delta N_{max}$ | Nu index |
|---|---|---|---|---|---|---|---|---|---|---|---|---|
| | −5.88 | 1.06 | 6.93 | 5.88 | −1.06 | 2.41 | −2.41 | 6.93 | 0.14 | 0.42 | 0.35 | 3.49 |

(NBO) charge, and atomic orbital coefficient of highest occupied molecular orbital (HOMO) indicated that N-atom is the nucleophilic center in piperidine (2) (Table 2).

The global and local chemical reactivity descriptors[49,50] were calculated from HOMO and lowest unoccupied molecular orbital (LUMO) energies of **(1a–h)** and (2) (Tables 3 and 4). The global descriptors were the ionization potential ($I_p$), electron affinity ($E_A$), the absolute electronegativity ($(I_P + E_A)/2$), chemical potential ($\mu = -\chi$), global hardness (η), and global softness ($S$) were calculated from $\eta = (E_{LUMO} - E_{HOMO})/2$ and $S = 1/2\eta$, respectively. While, the electrophilicity ($\omega$) can be calculated using the relation $\omega = \mu 2/2\eta$.[51–55] The global electrophilicity index measures the stabilization in energy when the system acquires an additional electronic charge ΔN from the environment.

Table 3 gives the energy of HOMO, energy of LUMO, chemical potential, hardness, softness, electrophilicity index and nucleophilicity index of piperidine (**2**).[56]. Domingo et al. had been reported a relative nucleophilicity index *Nu* using the relation $Nu = {}_{(Nu)}{}^{-\varepsilon HOMO(TCE)}$.[57,58,59,60] The values η and **Nu index** for piperidine (2) indicated that these parameters controlled their reactivities in the present reaction, equation (1). When two systems with different electronegativities react together, electrons are transferred from the nucleophilic molecule to the electrophilic molecule until the chemical potentials are equal.[61] The number of electrons transferred $\Delta N_{max}$ was calculated by the relation $\Delta N_{max} = -\mu/\eta$.[56]

The calculated energies and related molecular properties values of **(1a–h)** and the effective atomic charges, namely, Mulliken and NBO are given in Tables 4 and 5, respectively.[62]

The atomic charge values and atomic orbital coefficients are important in determining the reactivity of reaction centers toward nucleophilic attack.[62] Table 5 showed that (1) the naphthyl ipso carbon $C_1$ was more positively charged than the aryl ipso carbon $C_{1'}$ and (2) the interaction of a nucleophile with the naphthyl ipso carbon $C_1$ was controlled by its charge, while the reaction of the nucleophile with the aryl ipso carbon $C_{1'}$ was controlled by its coefficient. Thus, $C_{1'}$ could be considered as the high hard electrophilic center, while $C_1$ is the least one.

The mechanism for the piperidinolysis of ethers **(1a–h)** are studied theoretically using DFT methods at the B3LYP/6-311G(d,p) computational level.[48,63] The reaction process is initiated by the interaction between the two substrates (**1a–h**) and (**2**) followed by further

**Table 4.** Calculated energies and related molecular values of aryl 2,4-dinitronaphthyl ether (1a–h) by B3LYP/6-311G(d,p).

| | 1a | 1b | 1c | 1d | 1e | 1f | 1g | 1h |
|---|---|---|---|---|---|---|---|---|
| $\sigma$ | 0 | −0.27 | −0.17 | −0.07 | 0.12 | 0.23 | 0.37 | 0.78 |
| $E_{HOMO}$ | −6.86 | −6.16 | −6.59 | −6.72 | −6.40 | −6.84 | −7.00 | −7.48 |
| $E_{LUMO}$ | −3.22 | −3.15 | −3.19 | −3.19 | −3.16 | −3.35 | −3.32 | −3.53 |
| $\Delta E_e$ | 3.61 | 3.00 | 3.40 | 3.53 | 3.25 | 3.49 | 3.68 | 3.95 |
| $\mu$ (D) | 6.09 | 7.15 | 6.39 | 6.28 | 6.89 | 5.35 | 5.98 | 6.03 |
| $I_P$ | 6.84 | 6.16 | 6.59 | 6.73 | 6.41 | 6.84 | 7.01 | 7.48 |
| $E_A$ | 3.22 | 3.15 | 3.19 | 3.19 | 3.16 | 3.35 | 3.33 | 3.53 |
| $\mu$ (eV) | −5.03 | −4.65 | −4.89 | −4.96 | −4.78 | −5.09 | −5.17 | −5.50 |
| $\chi$ | 5.03 | 4.65 | 4.89 | 4.96 | 4.78 | 5.09 | 5.17 | 5.50 |
| $S$ | 0.55 | 0.67 | 0.59 | 0.57 | 0.62 | 0.57 | 0.54 | 0.51 |
| $\eta$ | 1.81 | 1.50 | 1.70 | 1.76 | 1.62 | 1.75 | 1.84 | 1.98 |
| $\omega$ | 7.00 | 7.21 | 7.03 | 6.96 | 7.03 | 7.42 | 7.25 | 7.67 |
| $\Delta N_{max}$ | 2.78 | 3.10 | 2.88 | 2.81 | 2.94 | 2.92 | 2.81 | 2.79 |

**Table 5.** Mulliken, NBO atomic charge, and atomic orbital coefficient of LUMO for the selected centers ($C_1$, $C_{1'}$) calculated by B3LYP/6–311G(d,p) for aryl 2,4-dinitronaphthalene ethers (**1a–h**).

| Mulliken atomic charges of **(1a–h)** | | | | | | | | |
|---|---|---|---|---|---|---|---|---|
| Atom | 1a | 1b | 1c | 1d | 1e | 1f | 1g | 1h |
| $C_1$ | 0.170 | 0.177 | 0.171 | 0.171 | 0.162 | 0.163 | 0.156 | 0.155 |
| $C_{1'}$ | 0.162 | 0.138 | 0.161 | 0.170 | 0.171 | 0.168 | 0.167 | 0.189 |
| NBO atomic charges | | | | | | | | |
| $C_1$ | 0.382 | 0.383 | 0.383 | 0.384 | 0.384 | 0.378 | 0.377 | 0.371 |
| $C_{1'}$ | 0.324 | 0.290 | 0.315 | 0.334 | 0.342 | 0.322 | 0.344 | 0.355 |
| Atomic orbital coefficient of LUMO | | | | | | | | |
| $C_1$ | 0.1912 | 0.1869 | 0.1900 | 0.1915 | 0.1928 | 0.1941 | 0.1950 | 0.1966 |
| $C_{1'}$ | 0.0078 | 0.0078 | 0.0079 | 0.0078 | 0.0078 | 0.0077 | 0.0076 | 0.0071 |

NBO: natural bond orbital; LUMO: lowest unoccupied molecular orbital.

steps which depended greatly on the stabilities of the possible activated complexes which explained whether the reaction is uncatalyzed or catalyzed either by SB or by SB-GA. The first step is the attack of the nucleophilic center in piperidine (2) on the more electrophilic C1 center in aryl naphthyl ethers (**1a–h**). The energy differences between the two possible HOMO/LUMO combinations for (**1a–h**) and piperidine (**2**) are given in Table 6. It showed that the $LUMO_{1a\text{-}h}$–$HOMO_2$ energy difference is lower than the $LUMO_2$- $HOMO_{1a\text{-}h}$ energy difference pointed out that the most favorable interaction was between the HOMO of (**1a–h**) and the LUMO of piperidine. Thus, **(1a–h)** behaved as an electrophile, while piperidine was a nucleophile.

The energy gap between the HOMO and LUMO is very important in determining the chemical reactivity of the molecule. The high value of the energy gap indicates that the molecule shows high chemical stability, while a small HOMO–LUMO gap means small

**Table 6.** Difference between the two possible HOMO/LUMO combinations for (1a–h) and piperidine (2).

| Descriptors | X = H, 1a | X = 4-$OCH_3$, 1b | X = 4-$CH_3$, 1c | X = 3-$CH_3$, 1d | X = 3-$OCH_3$, 1e | X = 4-Cl, 1f | X = 3-Cl, 1g | X = 4-$NO_2$, 1h |
|---|---|---|---|---|---|---|---|---|
| $E_{LUMO\,1a\text{-}h}$— $E_{HOMO\text{-}2}$ | 2.66 | 2.73 | 2.69 | 2.69 | 2.72 | 2.53 | 2.56 | 2.35 |
| $E_{LUMO\text{-}2}$— $E_{HOMO\text{-}1a\text{-}h}$ | 7.92 | 7.22 | 7.65 | 7.68 | 7.46 | 7.90 | 8.08 | 8.54 |

HOMO: highest occupied molecular orbital; LUMO: lowest unoccupied molecular orbital.

excitation energies to the manifold of excited states. The reported global parameters of ethers (**1a**–**h**),[62] such as electronic chemical potential $\boldsymbol{\mu}$ = –4.65 to –5.50 eV, was lower than that for piperidine **(2)**, ($\boldsymbol{\mu}$ = –2.41 eV), indicating that the net charge transfer **ΔN** takes place from the piperidine toward the **(1a**–**h)**. On the other hand, the electrophilicity index values of **(1a**–**h)** were in the range of 6.96–7.65 eV, a value that lies in the range of strong electrophile.[58] A good, more reactive, nucleophile is characterized by a lower value of, $\omega$ (0.42); and conversely, a good electrophile is characterized by a high value of $\omega$.[59] Table showed that 1h, 4-$NO_2$, has $\boldsymbol{\omega}$ = 7.67 and 1d, 4-$OCH_3$ has $\boldsymbol{\omega}$ = 6.96.

These parameters confirm that **(1a**–**h)** act as an electrophile, whereas piperidine acts as a nucleophile. The significant difference in electrophilicity ($\boldsymbol{\Delta\omega}$ = 6.56–7.13 eV) between piperidine and **(1a**–**h)** showed a high normal electronic demand (**NED**) polarity for this reaction.[28]

The local nucleophilic attack $f_{\mathbf{k}}^{+}$ Fukui functions (FFs) of N-atom in (2) and the local electrophilic centers attack $f_{\mathbf{k}}^{-}$ F of C1 in compounds **(1a**–**h)** were analyzed to predict the interaction between electrophilic center C1 and nucleophilic nitrogen atom in piperidinolysis reaction (equation (1)).

*Local reactivity descriptors.* FF[49] is one of the widely used local density functional descriptors to model chemical reactivity and site selectivity. The condensed FF of piperidine was calculated using the procedure proposed by Yang and Mortier[64] based on a finite difference method (equations (2)–(4)).

$$\boldsymbol{f+} = [\boldsymbol{q}(\boldsymbol{N+1})\text{-}\boldsymbol{q}(\boldsymbol{N})], \text{ for reaction with nucleophilic} \tag{2}$$

$$\boldsymbol{f-} = [\boldsymbol{q}(\boldsymbol{N})\text{-}\boldsymbol{q}(\boldsymbol{N\text{-}1})], \text{ for reaction with electrophilic} \tag{3}$$

$$\boldsymbol{f^0} = [\boldsymbol{q}(\boldsymbol{N+1})\text{-}\boldsymbol{q}(\boldsymbol{N\text{-}1})]/\boldsymbol{2}, \text{ for reaction with radical} \tag{4}$$

where $\boldsymbol{f_k}$ is the FF at atom **k** in a molecule and ($\boldsymbol{\alpha}$ = +, –,and 0) represents local philic quantities describing nucleophilic, electrophilic, and radical attacks, respectively. FFs $f^{+}(r)$, $f^{-}(r)$, and $f^{0}(r)$ were calculated using equations (2)–(4). The local electrophilicity and local nucleophilicity indices of a site $k$ in a molecule enable to predict the most favored nucleophilic–electrophilic attack of piperidine and **(1a**–**h)**. These indices could be calculated using the FFs,[58,65] equations (5)–(7), and cited in Tables 6 and 7.

$$\omega_k = \omega f_k^{+} \tag{5}$$

**Table 7.** The local electrophilicity, nucleophilicity, and maximum charge transfer in compounds (2).

| Piperidine (2) | $f_k^+$ | $f_k^-$ | $f_k^\circ$ | $\omega^+$ | $Nuf_k^+$ | $\Delta N_{max} f_k^+$ |
|---|---|---|---|---|---|---|
| $N_1$ | 0.26879 | −0.04254 | 0.226248 | 0.112892 | 0.938883 | 0.09327 |
| $C_2$ | −0.03527 | −0.09708 | −0.13235 | −0.01481 | −0.1232 | −0.01224 |
| $C_3$ | −0.01542 | −0.11309 | −0.12851 | −0.00648 | −0.05386 | −0.00535 |
| $C_4$ | −0.01158 | −0.07899 | −0.09057 | −0.00486 | −0.04045 | −0.00402 |
| $C_5$ | −0.01542 | −0.11309 | −0.12851 | −0.00648 | −0.05386 | −0.00535 |
| $C_6$ | −0.03527 | −0.09708 | −0.13235 | −0.01481 | −0.1232 | −0.01224 |

**Table 8.** FF ($\omega f_k^+$) and their local indices of $C_1$, $C_{1'}$ of (1a–h).

| Cpds | Atom | $f_k^+$ | $f_k^-$ | $f_k^\circ$ | $\omega^+$ |
|---|---|---|---|---|---|
| 1a | $C_1$ | −0.00723 | 0.09213 | 0.04245 | −0.05061 |
| | $C_{1'}$ | 0.01610 | −0.02951 | −0.00670 | 0.11270 |
| 1b | $C_1$ | −0.03443 | 0.09179 | 0.02868 | −0.24824 |
| | $C_{1'}$ | 0.04249 | −0.03132 | 0.00559 | 0.306353 |
| 1c | $C_1$ | −0.02053 | 0.09220 | 0.03584 | −0.14433 |
| | $C_{1'}$ | 0.02776 | −0.03004 | −0.00114 | 0.195153 |
| 1d | $C_1$ | −0.01553 | 0.09274 | 0.03861 | −0.10809 |
| | $C_{1'}$ | 0.01735 | −0.02943 | −0.00604 | 0.120756 |
| 1e | $C_1$ | −0.00794 | 0.09266 | 0.04236 | −0.05582 |
| | $C_{1'}$ | 0.00209 | −0.02803 | −0.01297 | 0.014693 |
| 1f | $C_1$ | −0.01275 | 0.09338 | 0.04031 | −0.09461 |
| | $C_{1'}$ | 0.01996 | −0.03110 | −0.00557 | 0.148103 |
| 1 g | $C_1$ | 0.00102 | 0.09327 | 0.04714 | 0.007395 |
| | $C_{1'}$ | 0.00829 | −0.02944 | −0.01058 | 0.060103 |
| 1 h | $C_1$ | 0.01216 | 0.08618 | 0.04917 | 0.093267 |
| | $C_{1'}$ | 0.00027 | −0.02674 | −0.01323 | 0.002071 |

$$Nu_k = Nu f_k^+ \tag{6}$$

The maximum charge transfer can be written as follows[57,59]

$$\Delta N_{max}(k) = \Delta N_{max} f_k^+ \tag{7}$$

The $f_k^+$ values indicated that the $N_1$ was the most nucleophile center of (2) and the nucleophilicity value of N1, $Nuf^+_k = 0.9389$, ensured that this atom was the most nucleophilic center compared with other atoms in piperidine (Table 5). On the other hand, the electrophilic attack $f^-_k$ of **(1a–h)** indicated that the $C_1$ or $C_{1'}$ carbon atom was the most electrophilic site of compounds **(1a–h)** ($f^+ C_1 = 0.452$). Recently, it was reported that the regioselectivity of nucleophile attack on **(1a–h)** was predominated on $C_1$ rather than $C_{1'}$.[62] Therefore, the FF values indicated that the most favorable nucleophile/electrophile interaction along the piperidinolysis reaction of **(1a–h)** occurred between the most electrophilic center $C_1$ carbon in **(1a–h)** and the nucleophilic N atom center in piperidine (equation (1)).

**Table 9.** Search for piperidine catalysis. Pseudo first-order ($k_{obs}$) and third-order rate constants ($k_N$) for the reaction of compounds ($1 \times 10^{-4}$ M/L) (1a–h) with piperidine (2) DMSO at 25°C.

| [Pip], mol/L/x | $10^3$ $k_{obs}$ $s^{-1}$ | | | | | | | |
|---|---|---|---|---|---|---|---|---|
| | **1a** | **1b** | **1c** | **1d** | **1e** | **1f** | **1g** | **1h** |
| 0.0010 | 0.59 | 0.64 | 1.18 | 0.65 | 1.08 | 1.24 | 1.31 | 2.00 |
| 0.0011 | 0.84 | 0.83 | 1.38 | 0.88 | 1.37 | 1.57 | 1.70 | 2.43 |
| 0.0012 | 1.13 | 1.08 | 1.58 | 1.18 | 1.70 | 1.87 | 2.05 | 2.82 |
| 0.0013 | 1.34 | 1.33 | 1.84 | 1.49 | 1.99 | 2.20 | 2.34 | 3.14 |
| 0.0014 | 1.72 | 1.52 | 2.11 | 1.70 | 2.28 | 2.46 | 2.71 | 3.59 |
| 0.0015 | 2.07 | 1.80 | 2.44 | 2.06 | 2.66 | 2.92 | 3.12 | 4.23 |
| **$k_N$ $L^2$ .$mol^{-2}$ $s^{-1}$** | 1170.0 | 918.5 | 1006.4 | 1121.3 | 1240.3 | 1299.9 | 1411.7 | 1706.7 |
| **$pk_a$** | 16.47 | 17.58 | 16.96 | 16.86 | 15.72 | 16.1 | 15.83 | 11.00 |
| **$\sigma^o$** | 0 | −0.12 | −0.15 | −0.07 | 0.13 | 0.27 | 0.37 | 0.82 |
| **$k_{rel} = k_x/k_H$** | 1 | 0.79 | 0.86 | 0.96 | 1.06 | 1.11 | 1.21 | 1.46 |

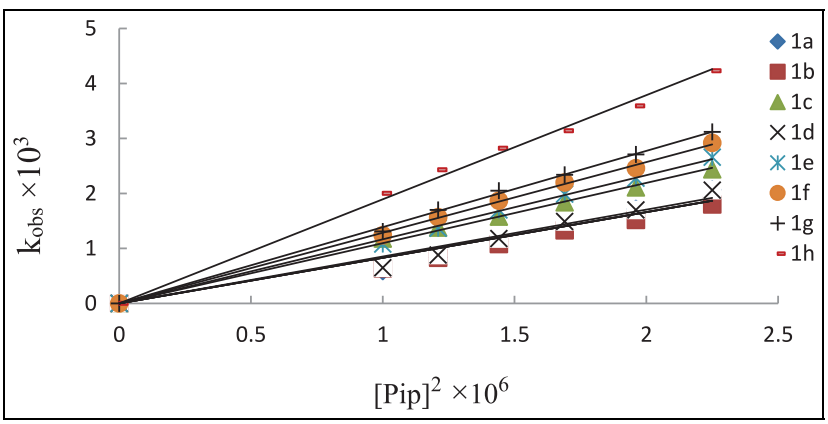


**Figure 2.** Plots showing linear dependence of $k_{obs}$ on $[piperidine]^2$ for the reaction of aryl 1-(2,4-dinitronaphthyl) ether (1a–h) with piperidine (2) at 25°C.

## *Experimental kinetic studies for the reaction of aryl 1-(2,4-dinitronaphthyl)ether (1a–h) with piperidine (2) in DMSO at 25°C*

The kinetic studies for the reaction of aryl 1-(2,4-dinitronaphthyl) ether **(1a–h)** with large excess of piperidine at 25°C were measured spectrophotometrically at $\lambda$ = 420 nm (Table 9). The spectra at completion reaction in all cases were identical to those of authentic samples of piperidino product **(3)** dissolved in DMSO with the same concentration of piperidine used in the kinetic runs. It is found that the values of the first-order rate constants, $k_{obs}$, increased linearly with $[piperidine]^2$ (Figure 2) indicated that the reaction is catalyzed by the second molecule of piperidine.

The third-order rate constants ($k_N$) at 25°C for the formation of the piperidino product **(3)** were determined from the slopes of the linear plots of $k_{obs}$ versus the $[piperidine]^2$ (Figure 2). Table 9 showed that ethers (1a–h) contain electron withdrawing substituents

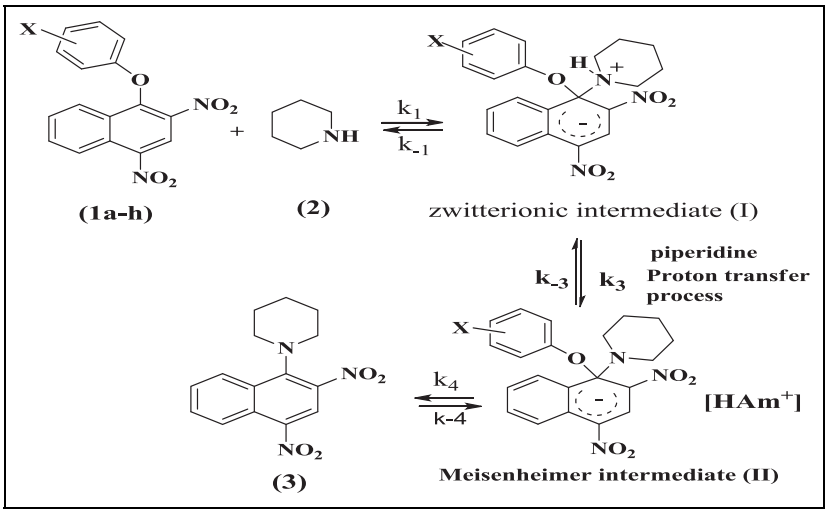


**Scheme 2.** Reaction of aryl 1-(2,4-dinitronaphthyl) ethers (1a–h) with piperidine (2).
**a,** X = H; **b**, X = 4-$OCH_3$; **c**, X = 4-$CH_3$; **d**, X = 3-$CH_3$; **e**, X = 3-$OCH_3$; **f**, X = 4-Cl; **g**, X = 3-Cl; and **h**, X = 4-$NO_2$.

enhance, while electron releasing substituents inhibit the rate and the effect of substituents followed the order: 4-$NO_2$ > 3-Cl > 4-Cl > 3-$OCH_3$ > H > 3-$CH_3$ > 4-$CH_3$ > 4-$OCH_3$. The values of $k_N$ showed relatively small dependence on the electronic effect of the substituent in the aromatic moiety of ethers (1a–h) pointing out that the electronic effect was inductive in nature.

The assignment of the piperidino product (**3**) and the third-order kinetics data suggested that the nucleophilic attack of piperidine $k_1$, on $C_1$ to give zwitterion intermediate **(I)** and the formation of product (3) occurred in fast steps. Therefore, the slow step was either deprotonation of zwitterion intermediate **(I)** (proton transfer process) to form the Meisenheimer ion **(II)**, that is, SB process or removing of phenoxide ion $k_4$, that is, SB-GA catalysis (**Scheme 2**).

The small $k_{rel}$ differences, shown in Table 9, in addition to the product analysis and order of the reaction proposed that the proton transfer step were slow. This suggestion was ensured by study the effect of addition external base, such as pyridine, or in the presence of conjugate acid, such as piperidinium hydrochloride. The catalysis is pronounced by the addition of external base pyridine, while the presence of conjugate piperidinium ion showed negligible change in rate constants for reaction of **(1b)** with piperidine (Table 10).[13,66,67] A result pointed out that the formation of zwitterion intermediate ($k_1$, $k_{-1}$) and the phenoxide ion expulsion to give the substitution product (3) were fast steps ($k_4$), and indicated that the proton transfer process was rate controlling step.

## *Rate equation for the reaction of ethers (1a–h) with piperidine (2) to form 1-piperidino-2,4-dinitronaphthalene (3)*

The overall rate equation (equation (8)) was derived according to **Scheme 2**, the catalyzed reaction, and the steady-state assumption.

**Table 10.** Pseudo first order ($k_{obs}$) and $k_{obs}$/[amine]$^2$ for the reaction of compound ($1 \times 10^{-4}$ M/L; 1b, X = 4-$OCH_3$) with piperidine ($1 \times 10^{-2}$ M) in presence of piperidinium hydrochloride and pyridine in DMSO at 25°C.

| [Piperidine], M | [Piperidinium hydrochloride], M | [Pyridine], M | $10^2$ $k_{obs}$ $s^{-1}$ | $k_{obs}$/[amine]$^2$ |
|---|---|---|---|---|
| 0.0010 | – | – | 0.0645 | 644.840 |
| 0.0011 | – | – | 0.0833 | 688.362 |
| 0.0012 | – | – | 0.1082 | 751.674 |
| 0.0013 | – | – | 0.1328 | 785.836 |
| 0.0014 | – | – | 0.1516 | 773.542 |
| 0.0015 | – | – | 0.1796 | 798.373 |
| 0.0010 | 0.001 | – | 0.0587 | 587.265 |
| 0.0011 | 0.001 | – | 0.0760 | 628.091 |
| 0.0012 | 0.001 | – | 0.0967 | 671.708 |
| 0.0013 | 0.001 | – | 0.1171 | 692.717 |
| 0.0010 | – | 0.0010 | 0.0745 | 744.637 |
| 0.0010 | – | 0.0012 | 0.1171 | 812.980 |
| 0.0010 | – | 0.0014 | 0.1735 | 885.167 |
| 0.0010 | – | 0.0016 | 0.2222 | 868.123 |
| $k_N$ $L^2.mol^{-2}s^{-1}$ | 850.98 | 958.34 | 918.5 | |

$$\frac{\mathbf{Rate}}{[\mathbf{ether}]} = k_{obs} = \frac{\mathbf{k}_1\mathbf{k}_3\mathbf{k}_4[\mathbf{piperidine}]^2[\mathbf{HAm}^+]}{(\mathbf{k}_{-3} + \mathbf{k}_4[\mathbf{HAm}^+])(\mathbf{k}_{-1} + \mathbf{k}_3[\mathbf{piperidine}])} \tag{8}$$

Since the third-order values was increased by addition of external base, therefore, the removing of the phenoxy (the $k_4$ step) was fast and equation (8) is reduced to equation (9)

$$k_N = \frac{\mathbf{k_{obs}}}{[\mathbf{piperidine}]^2} = \frac{\mathbf{k}_1\mathbf{k}_3}{\mathbf{k}_{-1}} \tag{9}$$

where $k_3$ is the third-order rate constant. Thus, proton transfer was rate determining step, $k_{-1} >> k_{Am}[Am]$ and $k_N$ equal $k_1k_3/k_{-1}$.

### *Structure–reactivity relationships*

*The application of Hammett concept.* The rate constants were correlated with different $\sigma^o$-Taft's constant values for substituted phenyl ring.[68] The $\sigma^o$-Taft's values represented inductive constants for substituted phenyl groups (–Ar) relative to the unsubstituted one $C_6H_5$–. Therefore, the electronic effect of the substituents in the leaving group moiety could be quantified by the use of a Hammett equation (10),[69] $\sigma^o$ is the substituent constant and ρ is the reaction constant.

$$\log k = \rho\sigma^o + \log k_o \tag{10}$$

Plot of log $k_N$ versus $\sigma^o$-Taft's[68] gave good straight line with ρ value of + 0.247 with correlation coefficients ($r$ = 0.91). The linearity of Hammett plot was a good evidence for the same mechanism for all substituents in the titled reactions, while '$\rho$' of + 0.247 pointed out a poor electronic effect of the substituent.[70]

The small positive value of ρ may be attributed to the compensation between the opposite charges in the activated state of the slow step between zwitterion (**I**) and Meisenheimer ion (**II**). Accordingly, equation (11) can be used to calculate the **ρ** value for the reaction.

$$\Delta\rho = (-\text{ve})\rho_{N^+} + (+\text{ve})\rho_{ArO^-} \tag{11}$$

And, the Hammett equation could be written in the form of equation (12).

$$\begin{aligned} log\frac{k_x}{k_o} &= \rho_{N^+}\sigma + \rho_{ArO^-}\sigma \\ log\frac{k_x}{k_o} &= \sigma^{\circ}(\rho_{N^+} + \rho_{ArO^-}) \end{aligned} \tag{12}$$

The small positive value of ρ showed that the activated state of the slow step was resembled to the product (Meisenheimer intermediate). It has been reported that the high **ρ** values ( > 2) indicated that the departure of the aryl leaving group is slow,[71] while the small value of ρ values (0.34–0.25) indicated fast departure of the aryl leaving group. Hence, the low positive of **ρ** value for the present reaction indicated that the proton transfer process is the rate controlling step.

*The application of Brønsted concept.* The magnitude of the Brønsted coefficient has usually been related to the extent of bond formation in the activated complex that involved in the slow step (equation (13)).[72]

$$\log k_N{}^{25} = \beta \ \log K_a + \text{ constant.} \tag{13}$$

The magnitude and the sign of Brønsted coefficient ($\beta$) was reported to depend on the p*Ka* either for attacking nucleophile or the leaving group.[73,74] As the p*Ka* of the nucleophile varied with constant leaving group a positive Brønsted coefficient ($\beta_N$) is observed.[24,32] On the other hand, the change of the p*Ka* values of the leaving group with constant nucleophile would result in a negative Brønsted coefficient ($\beta_{lg}$)[30] due to the inverse proportionality between p*Ka* of the leaving group and the rate.

Table 7 showed that the reactivity of **(1a–h)** toward piperidine increased with the decrease in p*Ka* of the leaving aryloxide anion group.[74,75] The small and negative sign of $\beta_{lg}$ value (–0.04, $r$ = 0.77) indicated that the activated complex involved in the slow step is significantly associative and product-like, that is, Meisenheimer intermediate, implying a very late transition state.[74,76] Both $\beta$lg and ρ values support that the activated complex involved in the slow step was product-like.

## *Computational studies of mechanism for the reaction of phenyl 1-(-2,4-dinitronaphthyl) ether (1a) with piperidine (2)*

The identification of transition states and their existence were confirmed by the presence of a single imaginary frequency in the Hessian matrix.[77–79] The kinetic results proved that the substitution reaction was overall third order and catalyzed by the second molecule of piperidine, that is, SB-GA (Scheme 2). Therefore, the mechanism pathway was rewritten to show the fine processes (**Scheme 3**). The nucleophile attacks $C_1$ to form **TS (1)** which was going to

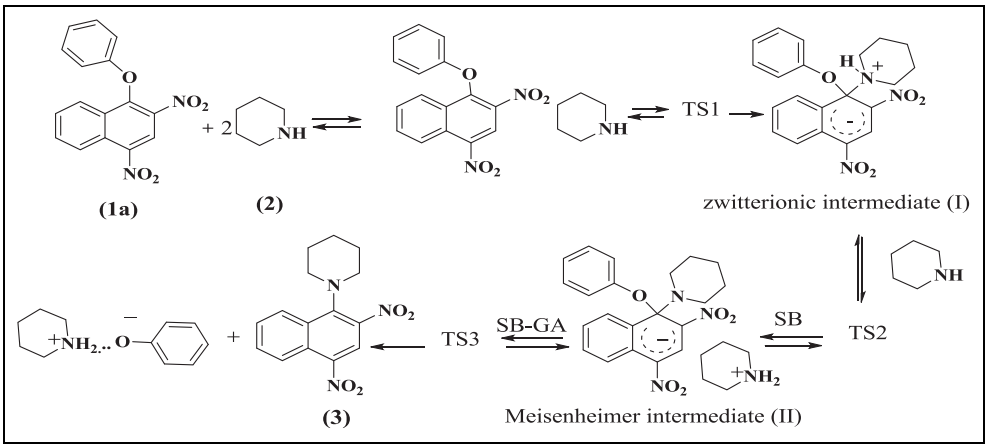


**Scheme 3.** The mechanism of ether (1a) with piperidine (2).

zwitterion intermediate **(I)** in fast step. The slow step proceeded by two possible pathways, first, the zwitterionic intermediate **(I)** underwent deprotonation to form the Meisenheimer intermediate (II) $k_{-3}$ in the RDS through **TS (2)** and rapid removing of leaving group, $k_4$, that is, SB catalysis. Second, zwitterionic intermediate **(I)** underwent fast proton transfer with slow expulsion of phenoxide ion $k_4$ through **TS (3)** to give the substitution product (RDS), that is, SB-GA catalysis.

*Energy profile and geometrical analyses of activated complexes involved in the piperidinolysis of (1a–h).* The theoretical mechanism of catalyzed reaction, the energies of the reactants, the products, and the activated states were calculated by DFT methods were determined (Figure 3). It expressed the possible activated complexes for the reaction of (**1a**) with piperidine. The same method was used to calculate the bond lengths and bond angles of activated complexes involve in the reaction (Table 11).

The bond length of $C_1$–$O_{11}$ of zwitterion intermediate (**I**) (Figure 4(b)) became slightly larger than the same bond in **TS1** (Figure 4(a)). Table 11 revealed that the new $C_1$–$N_{1''}$ bond length became more shorter in ZI(I) than the same bond in **TS1**. This result clearly showed that $C_1$–$O_{11}$ bond begin to break and $C_1$–$N_{1''}$ bond started to be formed.

The bond lengths of $C_1$–$O_{11}$ and $C_1$–$N_{1''}$ in TS2 had the same bond lengths as those in zwitterion intermediate **(I)** (Figure 4(b)). While there was gradual increase in $C_1$–$O_{11}$ and decrease in $O_{11}$–$N_{1''}$ bond lengths in the Meisenheimer intermediate **(II)** (Figure 4(d) and Table 11). The last TS3 (Figure 4(d)) showed that $C_1$–$O_{11}$ has a maximum increase in bond length whereas that of $C_1$–$N_{1''}$ became the shortest distance. According to the gradual changes in $C_1$–$O_{11}$ and $C_1$–$N_{1''}$ in all activated complexes suggest that **TS2** is the important activated complex and its formation is the RDS. Also, the value of the bond angle $C_1$–$O_{11}$–$N_{1''}$ was around 89–106.4$^{o}$ indicated that the reaction started by perpendicular attack of piperidine on $C_1$ of compound **(1)**.

Energy values of the possible activated complexes shown in Figure 4 were depicted in Table 12. The activation energies of all species and compounds in the reaction of **1a** with

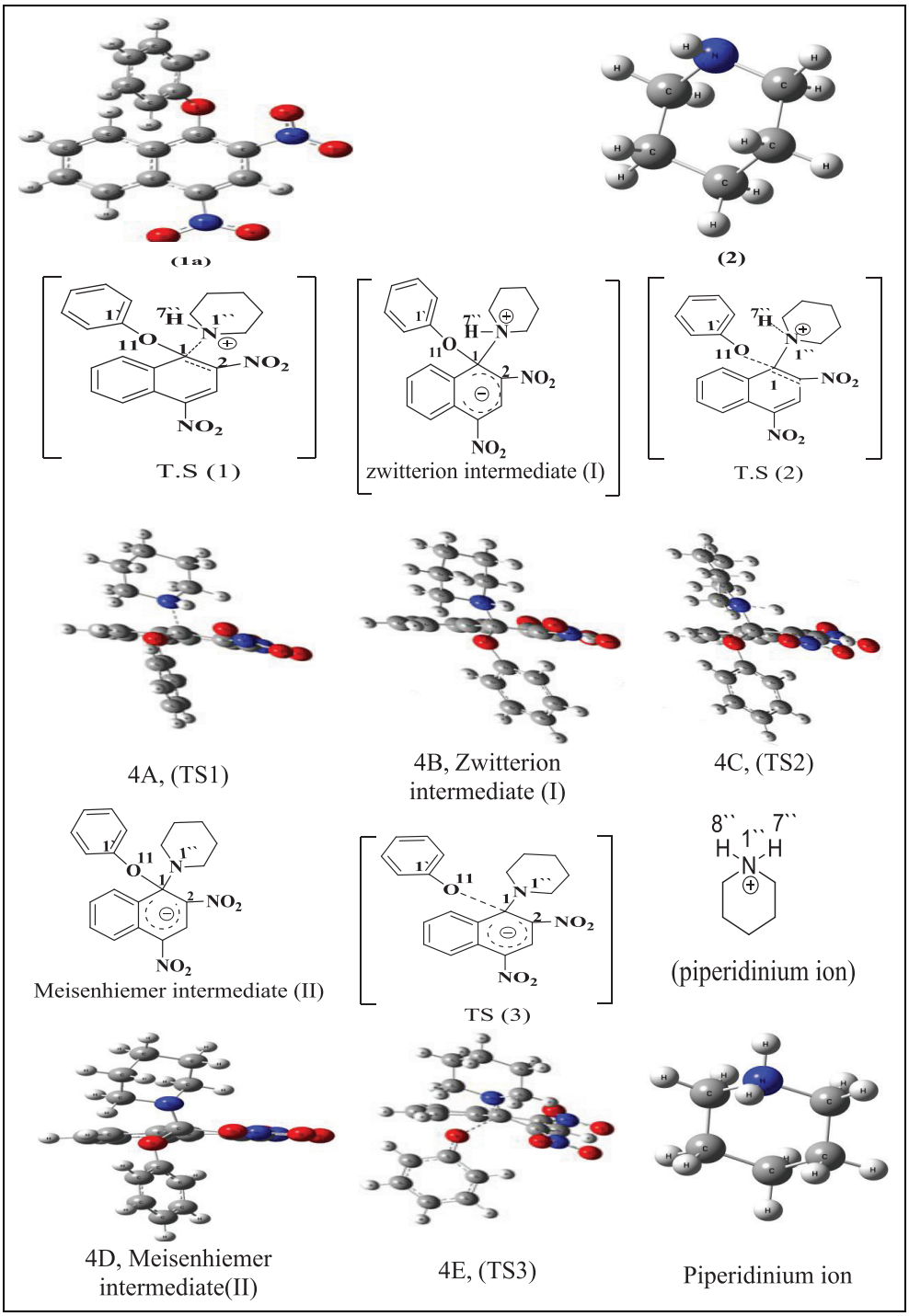


**Figure 3.** B3LYP/6-311G(d,p) optimized geometries of the transition states and intermediates involved in the piperidinolysis of (1a–h) in DMSO.

**Table 11.** B3LYP/6-311G(d,p) optimized geometries of bond length, bond angles, and of the reactants, products, intermediates, and transition states for the reaction of ether (1a) and piperidine (2) in (a) vacuum and (b) DMSO. Distances are given in angstroms.

| Species | Bond lengths (Å) | | | Bond angles (°) | | |
|---|---|---|---|---|---|---|
| | BL | Vacuum | DMSO | BA | Vacuum | DMSO |
| (1a) + 2(2) | $C_I$–$O_{II}$ | 1.361 | 1.360 | $C_I$–$O_{II}$–$C_{I'}$ | 121.3° | 121.2° |
| | $C_{I'}$–$O_{II}$ | 1.395 | 1.396 | $O_{II}$–$C_I$–$C_2$ | 122.3° | 122.2° |
| (1a) + (2) | $C_I$–$O_{II}$ | 1.361 | 1.360 | $C_I$–$O_{II}$–$C_{I'}$ | 121.3° | 121.2° |
| | $C_{I'}$–$O_{II}$ | 1.395 | 1.396 | $O_{II}$–$C_I$–$C_2$ | 122.3° | 122.2° |
| TS (I) | $C_I$–$O_{II}$ | 1.403 | 1.384 | $C_I$–$O_{II}$–$C_{I'}$ | 120.0° | 120.7° |
| | $C_{I'}$–$O_{II}$ | 1.394 | 1.393 | $O_{II}$–$C_I$–$N_{I''}$ | 93.2° | 90.9° |
| | $C_I$–$N_{I''}$ | 1.867 | 2.048 | $O_{II}$–$C_I$–$C_2$ | 118.5° | 120.4° |
| ZI (I) | $C_I$–$O_{II}$ | 1.430 | 1.430 | $C_I$–$O_{II}$–$C_{I'}$ | 119.7° | 122.7° |
| | $C_{I'}$–$O_{II}$ | 1.399 | 1.385 | $O_{II}$–$C_I$–$N_7$ | 100.8° | 100.8° |
| | $C_I$–$N_{I''}$ | 1.470 | 1.470 | | | |
| TS2 | $C_I$–$O_{II}$ | 1.430 | 1.401 | $C_I$–$O_{II}$–$C_{I'}$ | 122.1° | 122.2 |
| | $C_{I'}$–$O_{II}$ | 1.384 | 1.384 | $O_{II}$–$C_I$–$N_{I''}$ | 106.4° | 105.9 |
| | $C_I$–$N_{I''}$ | 1.470 | 1.577 | | | |
| MC (II) | $C_I$–$O_{II}$ | 1.430 | 1.430 | $C_I$–$O_{II}$–$C_{I'}$ | 123.4° | 123.6° |
| | $C_{I'}$–$O_{II}$ | 1.363 | 1.369 | $O_{II}$–$C_I$–$N_{I''}$ | 103.0° | 103.1° |
| | $C_I$–$N_{I''}$ | 1.495 | 1.493 | | | |
| TS3 | $C_I$–$O_{II}$ | 2.346 | 2.265 | $C_I$–$O_{II}$–$C_{I'}$ | 131.3° | 128.2° |
| | $C_I$–$O_{II}$ | 1.299 | 1.301 | $O_{II}$–$C_I$–$N_{I''}$ | 089.6° | 94.8° |
| | $C_I$–$N_{I''}$ | 1.359 | 1.343 | | | |
| (3) | $C_I$–$N_{I''}$ | 1.402 | 1.383 | $N_I$–$C_I$–$C_2$ | 121.9° | 124.3° |
| Piperidinium ion | $N_{I''}$–$H_{I''}$ | 1.027 | 1.026 | $H_{I''}$–$N_{I''}$–$H_{I'''}$ | 106.2° | 105.6° |
| | $N_{I''}$–$H_{I'''}$ | 1.026 | 1.025 | | | |
| (2) | $N_{I''}$–$H_{I''}$ | 1.021 | 1.021 | | | |
| $PhO^-$ | $C_I$–$O_{II}$ | 1.266 | 1.279 | | | |
| PhOH | $C_I$–$O_{II}$ | 1.369 | 1.369 | $C_{I'}$–$O_{II}$–$H_{12}$ | 108.8° | 109.2° |
| | $C_I$–$H_{12}$ | 0.969 | 0.971 | | | |

DMSO: dimethyl sulfoxide.

piperidine were compute in both gas and DMSO phases, that is from substrate **(1)** → **TS1** → **(I)** → **TS2** → **(II)** (**(II)pipH** $^+$ ) **TS3** (**TS3pipH** $^+$ ) **(3)** (Table 12). The energy change (**ΔE**) of the reaction of **(1a)** with piperidine follows the order of **TS2-(II)** > **(II)-TS3** > **TS2-(I)** > **TS1-(I)**. When the energies of activated complexes **(II)pipH** $^+$ and **TS3pipH** $^+$ were taking into consideration, the energy change followed the order **TS2-(II)pipH** $^+$ > **(II)pipH** $^+$ **-TS3pipH** $^+$ > **(I)-TS2** > **TS1-(I)**. Both considerations led to suggestion that the proton transfer process was the RDS. These orders were completely consistent with experimental results.

## Conclusion

The reaction of aryl 1-(2,4-dinitronaphthyl) ether (**1a**–**h**: **a**, X = H; **b**, X = 4-$OCH_3$; **c**, X = 4-$CH_3$;**d**, X = 3-$CH_3$; **e**, X = 3-$OCH_3$;**f**, X = 4-Cl; **g**, X = 3-Cl; and **h**, X = 4-$NO_2$) with piperidine in DMSO gave 1-piperidino-2,4-dinitronaphthalene and substituted phenol

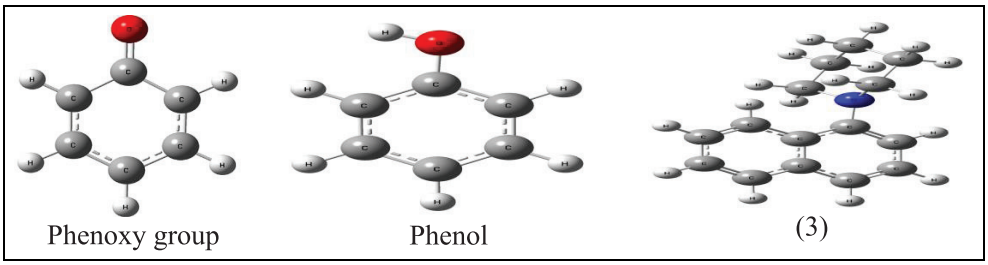


**Figure 4.** Pictures of the ether (1a), phenol, and phenoxide anion in DMSO.

**Table 12.** Energy (in hartree/particle) of the reactants, products, intermediates, and transition states for the reaction of ether (1a) and piperidine (2) in (a) vacuum and (b) DMSO.

| Species | Energy (in hartree/particle) | |
|---|---|---|
| | Vacuum | DMSO |
| (1a) + 2(2) | −1604.9451 | −1604.9642 |
| (1a) + (2) | −1353.0412 | −1353.0570 |
| TS (I) | −1353.0315 | −1353.0504 |
| ZI (I) | −1353.0254 | −1353.0505 |
| TS(2) | −1352.9642 | −1352.9856 |
| MC (II) | −1352.5119 | −1352.5841 |
| TS(3) | −1352.4862 | −1352.5622 |
| Product (3) | −1045.5770 | −1045.5882 |
| Piperidinium ion | −252.2859 | −252.3721 |
| Piperidine (2) | −307.4649 | −307.4712 |
| $PhO^-$ | −306.8842 | −306.9745 |
| PhOH | −307.4649 | −307.4712 |
| MC(II) + piperidinium | −1604.7979 | −1604.9561 |
| TS3 + piperidinium | −1604.7722 | −1604.9343 |
| (2) + (3) + phenol | −1604.9458 | −1604.9666 |

DMSO: dimethyl sulfoxide.

with no side products. The substitution was considered regioselective reaction because the piperidine attached itself to the ipso carbon atom of naphthyl moiety. Kinetic studies indicated that the reaction was third order, where the second piperidine molecule acted as a catalyst. It was found that electron withdrawing substituents enhanced while electron releasing substituents inhibited the rate. The linearity of Hammett plot was a good evidence for the same mechanism for all substituents, while its magnitude indicated poor electronic effect of the substituent. The magnitude and the sign of Brønsted coefficient ($\beta$) showed that the reactivity of **(1a–h)** toward piperidine increased with the decrease in p*Ka* of the aryloxide leaving group The small and negative sign of $\beta_{lg}$ value indicated that the activated complex involved in the slow step is significantly associative and Meisenheimer intermediate-like. The optimized geometric parameters (bond lengths and angles) of piperidine by BLYP with 6-311G(d,p) was consistent with those reported earlier. The values of Mulliken charge, NBO charge, and atomic orbital coefficient of HOMO indicated that N-atom is the nucleophilic

center in piperidine. Mulliken charge, NBO charge, and atomic orbital coefficients parameters of (**1a**–**h**) indicated that the naphthyl ipso carbon $C_1$ is more positively charged than the aryl ipso carbon $C_{1'}$. The energy difference between the two possible HOMO–LUMO combinations and the net charge transfer $\Delta N$ pointed out that (**1a**–**h**) behaves as an electrophile, while piperidine was a nucleophile. The local parameters $f_k^{+}$ and $Nuf^{+}{}_k$ values indicated that the $N_1$ is the most nucleophile center of piperidine, while the electrophilic attack $f_k$ of (**1a**–**h**) indicated that the $C_1$ or $C_{1'}$ carbon atom is the most electrophilic site of compounds (**1a**–**h**). The correct pathway mechanism was achieved by calculating the energies of the reactants, the products and the activated complexes energies as well as their bond lengths and bond angles. The gradual changes in $C_1$–$O_{11}$ and $C_1$–$N_{1''}$ as well as the energies of all activated complexes involved in the reaction suggest that TS2 was the important activated complex and its formation is presumably the RDS. This was in agreement with the experimental kinetic results. Also, the value of the bond angle $C_1$–$O_{11}$–$N_{1''}$ was around 89–106.4° indicating that the reaction was starting by perpendicular attack of piperidine on $C_1$ of compound (1a) to form TS1.

## Declaration of conflicting interests

The author(s) declared no potential conflicts of interest with respect to the research, authorship, and/or publication of this article.

## Funding

The author(s) received no financial support for the research, authorship, and/or publication of this article.

## ORCID iD

Mohamed A El-Atawy https://orcid.org/0000-0002-5042-5221

## References

1. Bunnett JF and Zahler RE. *Chem Rev* 1951; 49: 273–412.
2. Emokpae TA, Uwakwe PU and Hirst J. *J Chem Soc Perkin Trans* 1993; 2: 125–132.
3. Hirst J. *J Phys Organ Chem* 1994; 7: 68–79.
4. Nudelman NS and Palleros D. *J Chem Soc Perkin Trans* 1984; 2: 1277–1280.
5. Terrier F. *Nucleophilic aromatic displacement*. Weinheim: VCH Publishers, 1991.
6. Bernasconi CF, Muller MC and Schmid P. *J Organ Chem* 1979; 44: 3189–3196.
7. Ayediran D, Bamkole TO, Hirst J, et al. *J Chem Soc Perkin Trans* 1977; 2: 1580–1583.
8. Bunnett J, Bernasconi C. *J Am Chem Soc* 1965; 87: 5209–5218.
9. Bunnett JF and Sekiguchi S, Smith LA. *J Am Chem Soc* 1981;103: 4865–4871.
10. Chamberlin RA and Crampton MR. *J Chem Soc Perkin Trans* 1994; 2: 425–432.
11. Chamberlin RA and Crampton MR. *J Chem Soc Perkin Trans* 1995; 2: 1831–1838.
12. Hirst J and Onyido I. *J Chem Soc Perkin Trans* 1984; 2: 711–715.
13. Sekiguchi S, Hosokawa M, Suzuki T, et al. *J Chem Soc Perkin Trans* 1993; 2: 1111–1118.
14. Orvik JA and Bunnett J. *J Am Chem Soc* 1970; 92: 2417–2427.
15. Fujinuma H, Hosokawa M, Suzuki T, et al. *Bullet Chem Soc Japan* 1989; 62: 1969–1975.
16. Crampton MR and Routledge PJ. *J Chem Soc Perkin Trans* 1984; 2: 573–581.
17. Hasegawa Y. *Bullet Chem Soc Japan* 1983; 56: 1314–1318.

18. Hasegawa Y. *J Chem Soc Perkin Trans* 1985; 2: 87–92.
19. Ayediran D, Bamkole TO and Hirst J. *J Chem Soc Perkin Trans* 1976; 2: 1396–1398.
20. Hamed EA. *Int J Chem Kinetic* 1997; 29: 599–605.
21. Hamed EA. *Int J Chem Kinetic* 1997; 29: 515–521.
22. Hamed E, El–Bardan A, Saad E, et al. *J Chem Soc Perkin Trans* 1997; 2: 2415–2422.
23. El-Bardan AA, El-Subruiti GM, El-Hegazy FEZM, et al. *Int J Chem Kinetic* 2002; 34: 645–650.
24. EL Hegazy FEZM, Abdel Fattah SZ, Hamed EA, et al. *J Phys Organ Chem* 2000; 13: 549–554.
25. Fathalla MF, Ibrahim MF and Hamed EA. *J Chem Res* 2004; 2004: 150–151.
26. Hamed E. *J Chem Res* 2006; 7: 413–416.
27. Al–Howsaway HO, Fathalla MF, El–Bardan AA, et al. *J Chem Res* 2007; 2007: 509–512.
28. Asghar BH, Fathalla MF and Hamed EA. *Int J Chem Kinetic* 2009; 41: 777–786.
29. Khattab SN, Hassan SY, Hamed EA, et al. *Bullet Korean Chem Soc* 2010; 31: 75–81.
30. Khattab SN, Hamed EA, Albericio F, et al. *Bullet Chem Soc Japan* 2011; 84: 633–639.
31. Khattab SN, Kharaba MA, El–Hawary A, et al. *Open J Physical Chem* 2012; 2: 156.
32. Ibrahim MF, El-Atawy MA, El-Sadany SK, et al. *Int J Chem Kinetic* 2013; 45: 551–559.
33. Hamed EA and Youssef IS. *The kinetics Studies of the Reactions of 1–Chloro–2,4–dinitronaphthalene with some Substituted Anilines*. PhD Thesis, Alexandria University, Alexandria, Egypt, 2016.
34. Senger NA, Bo B, Cheng Q, et al. *J Organ Chem* 2012; 77: 9535–9540.
35. Fernandez DRB, Elsegood MR, Fairley G, et al. *Europ J Organ Chem* 2016: 5238–5242.
36. Frisch MJ, Trucks GW, Schlegel HB, et al. *Gaussian 09 ed*. Wallingford, CT: Gaussian Inc, 2009.
37. Dennington R, Keith T and Millam J. Gauss View, Version 5. Shawnee, KS: Semichem, 2009.
38. Carballeira L and Pérez–Juste I. *J Comput Chem* 1998; 19: 961–976.
39. Gundersen G and Rankin DW. *Acta Chem Scand Ser A* 1983; 37: 865–874.
40. Güllüoglu MT and Yurdakul Ş. *Vibrat Spectroscop* 2001; 25: 205–211.
41. Hirokawa T, Kimura T, Ohno K, et al. *Spectrochim Acta Part A: Mol Spectroscop* 1980; 36: 329–332.
42. Marcotrigiano G, Menabue L and Pellacani GC. *J Mol Struct* 1976; 30: 85–94.
43. Okishi Y, Imai Y and Aida K. *J Inorgan Nuclear Chem* 1973; 35: 101–107.
44. Titova T, Anisimova O and Pentin YA. *Optic Spectros* 1967; 23: 495.
45. Vedal D, Ellestad O, Klaboe P, et al. *Spectrochim Acta Part A: Mol Spectroscop* 1976; 32: 877–890.
46. Vayner E and Ball D. *J Mol Struct* 2000; 496: 175–183.
47. Güllüoğlu MT, Erdoğdu Y and Yurdakul Ş. *J Mol Struct* 2007; 834: 540–547.
48. Lee C, Yang W and Parr R. *Phys Rev vol B* 1988; 37: 785–789.
49. Ayers PW and Levy M. *Theor Chem Account* 2000; 103: 353–360.
50. Geerlings P, De Proft F and Langenaeker W. *Chem Rev* 2003; 103: 1793–1874.
51. Elliott P, Burke K, Cohen MH, et al. *Phys Rev A* 2010; 82: 024501.
52. Padmanabhan J, Parthasarathi R, Subramanian V, et al. *J Phys Chem A* 2007; 111: 1358–1361.
53. Chattaraj PK and Giri S. *J Phys Chem A* 2007; 111: 11116–11121.
54. Parr RG, Szentpály LV and Liu S. *J Am Chem Soc* 1999; 121: 1922–1924.
55. Flippin LA and Gallagher DW, Jalali–Araghi K. *J Organ Chem* 1989; 54: 1430–1432.
56. Parr RG and Yang W. *J Am Chem Soc* 1984; 106: 4049–4050.
57. Domingo LR, Pérez P and Sáez JA. *RSC Adv* 2013; 3: 1486–1494.
58. Domingo LR, Aurell MJ, Pérez P, et al. *Tetrahedron* 2002; 58: 4417–4423.
59. Domingo LR, Chamorro E and Perez P. *J Phys Chem A* 2008; 112: 4046–4053.
60. Ghomri A and Mekelleche S. *J Mol Struct* 2010; 941: 36–40.
61. Pérez P, Domingo LR, Duque–Noreña M, et al. *J Mol Struct* 2009; 895: 86–91.
62. Moghazi YM, Fathalla MF, Hamada NMM, et al. *Int J Chem Kinet* 2020; 52: 341–355.
63. Becke AD. *J Chem Phys* 1993; 98: 5648–5652.
64. Yang W and Mortier WJ. *J Am Chem Soc* 1986; 108: 5708–5711.
65. Pérez P, Domingo LR and Aurell MJ, *Tetrahedron* 2003; 59: 3117–3125.

66. Crampton MR and Gibson B. *J Chem Soc Perkin Trans* 1981; 2: 533–539.
67. Crampton MR and Greenhalgh C. *J Chem Soc Perkin Trans* 1983; 2: 1175–1178.
68. Taft RW Jr. *J Phys Chem* 1960; 64: 1805–1815.
69. Johnson CD and Johnson CD. *The Hammett Equation*. Cambridge: Cambridge University Press, 1973.
70. Pietra F. *Quart Rev Chem Soc* 1969; 23: 504–521.
71. Chaw Z, Fischer A and Happer D. *J Chem Soc B: Phys Organ* 1971; 1818–1819.
72. Mohanty TR and Nayak PL. *J Chem Soc Perkin Trans* 1975; 2: 242–244.
73. Senatore L, Ciuffarin E and Fava A. *J Am Chem Soc* 1970; 92: 3035–3039.
74. Jover J, Bosque R and Sales J. *Qsar Combin Sci* 2007; 26: 385–397.
75. Hudson R and Klopman G. *J Chem Soc* 1962; 1062–1067.
76. Ibrahim MF, Abdel–Reheem HA, Khattab SN, et al. *Int J Chem* 2013; 5: 33–45.
77. Wiberg KB. *Tetrahedron* 1968; 24: 1083–1096.
78. Reed AE, Weinstock RB and Weinhold F. *J Chem Phys* 1985; 83: 735–746.
79. Reed AE, Curtiss LA and Weinhold F. *Chem Rev* 1988; 88: 899–926.